Electronic Supplementary Material (ESI) for Inorganic Chemistry Frontiers.

Supplementary Information

Guest dependent reversible single-crystal to single-crystal structural transformation in a flexible Gd(III)-coordination polymer

Tapan K. Pal, Dinesh De, Subhadip Neogi and Parimal K. Bharadwaj*

Department of Chemistry, Indian Institute of Technology Kanpur, 208016, India

Email: pkb@iitk.ac.in

Contents

Synthesis of the complexes.

$\{[Gd_2(L)_3(DMF)_4]\cdot 4DMF\cdot 3H_2O\}_n$ (1): Compound **1** has been synthesized according to the reported procedure from our group. A mixture of $Gd(NO_3)_3\cdot 6H_2O$ (0.5 mmol), H_2L (0.5 mmol) were taken in DMF (10 mL) and ethanol (5 mL) and heated to 100 °C under autogenous pressure in a Teflon-lined steel bomb for 2 days, followed by slow cooling (5° C h^{-1}) to room temperature. The yellowish block-shaped crystals formed were collected, washed with DMF and preserved in dried DMF. Yield: 64%; IR (KBr cm^{-1}): 3397(br), 3085 (m), 2933 (m), 2880 (w), 1675 (s), 1631 (s), 1543 (s), 1461 (m), 1387 (s), 1341 (s), 1253 (w), 1187(w), 1093 (m), 1062 (w); Anal. calcd. for $C_{66}H_{74}N_{20}O_{47}Gd_2$: C, 35.80, H, 3.36, N, 12.65%; found: C, 35.71, H, 3.52, N, 12.58%.

$\{[Gd_2(L)_3(DMF)_4]\cdot(4\text{-ClPhCHO})\cdot 4DMF\}_n$ (1a): Crystals of **1** were kept inside a saturated dichloromethane solution of 4-chlorobenzaldedhyde (~ 200mg of aldehyde in 3ml DCM solution) for 5 days, which afforded compound **1a**. Anal. calcd. for $C_{73}H_{73}ClN_{20}O_{45}Gd_2$: C, 38.12; H, 3.20; N, 12.18%. Found: C, 37.99; H, 3.15; N, 12.46%. IR(KBr, cm^{-1}): 3396(br), 2933(m), 1700(s), 1650.54(s), 1595(m), 1538(s), 1341(s), 1187(s), 1109(s), 921.93(s), 800(s), 725(s), 678(s).

$\{[Gd(L)_{1.5}(DMF)(H_2O)_3]\cdot(4\text{-FPhCHO})\cdot(DMF)\cdot 3(H_2O)\}_n$ (1b): Single crystals of **1** upon exposure to vapor of 4-fluorobenzaldehyde for 5 days afforded compound **1b** without any loss in crystallinity. Anal. calcd. for $C_{34}H_{37}FN_8O_{27}Gd$: C, 35.03; H, 3.20; N, 9.61%. Found: C, 35.23; H, 3.15; N, 9.92%. IR (KBr, cm^{-1}): 3410(br), 2937.14(m), 1706(s), 1649.68(s), 1548(m), 1506(s), 1454(s), 1342(s), 1150(m), 1108(s), 922(s), 860(s), 800(m), 726(s), 677(s).

$\{[Gd(L)_{1.5}(DMF)(H_2O)_3]\cdot(4\text{-MePhCHO})\cdot 2(DMF)\cdot(H_2O)\}_n$ (1c): Single crystals of **1** upon exposure to vapor of 4-methylbenzaldehyde for 5 days afforded compound **1c** without a loss in crystallinity. Anal. calcd. for $C_{38}H_{42}N_9O_{26}Gd$: C, 38.10; H, 3.53; N, 10.52%. Found: C, 38.25; H,

3.45; N, 10.45%. IR (KBr, cm^{-1}): 3416(br), 2936(m), 1695(s), 1650(s), 1604(m), 1537(s), 1454(s), 1385(s), 1343(s), 1216(m), 1109(s), 923(s), 767(s), 846(s).

Table S1. Selected Bond Distances (Å) and Bond Angles (°) of **1a-1c**.

1a

Gd(1)-O(2) 2.356(3)	Gd(1)-O(38) 2.360(4)	Gd(1)-O(18) 2.395(3)
Gd(1)-O(13) 2.397(3)	Gd(1)-O(45) 2.406(3)	Gd(1)-O(37) 2.408(4)
Gd(1)-O(46) 2.437(3)	Gd(1)-O(28) 2.500(3)	Gd(1)-O(11) 2.719(3)
Gd(2)-O(11) 2.350(3)	Gd(2)-O(35) 2.354(4)	Gd(2)-O(36) 2.369(4)
Gd(2)-O(12) 2.408(3)	Gd(2)-O(19) 2.414(3)	Gd(2)-O(29) 2.482(3)
Gd(2)-O(30) 2.490(3)	Gd(2)-O(1) 2.504(3)	Gd(2)-O(2) 2.631(3)

O2 Gd1 O18 83.18(12)	O38 Gd1 O18 74.51(13)	O2 Gd1 O13 72.40(12)
O38 Gd1 O13 142.37(12)	O18 Gd1 O13 133.50(12)	O2 Gd1 O45 122.97(12)
O38 Gd1 O45 80.01(13)	O18 Gd1 O45 78.82(12)	O13 Gd1 O(45) 82.24(12)
O2 Gd1 O37 73.95(13)	O38 Gd1 O37 72.56(13)	O18 Gd1 O37 71.16(13)
O13 Gd1 O37 133.74(13)	O45 Gd1 O37 143.57(13)	O2 Gd1 O46 89.82(12)
O38 Gd1 O46 92.72(13)	O18 Gd1 O46 145.02(12)	O13 Gd1 O46 75.12(12)
O45 Gd1 O46 131.81(12)	O37 Gd1 O(46) 73.96(13)	O2 Gd1 O28 132.31(12)
O38 Gd1 O28 74.49(12)	O18 Gd1 O28 144.48(12)	O13 Gd1 O28 69.72(12)
O45Gd1O28 79.15(12)	O37 Gd1O28 114.75(13)	O46Gd1O28 53.27(12)
O2 Gd1 O11 72.75(11)	O38 Gd1 O11 120.84(12)	O18 Gd1 O11 66.96(11)
O13 Gd1 O11 68.21(11)	O45 Gd1 O11 50.36(11)	O37 Gd1 O11 128.57(12)
O46 Gd1 O11 142.62(11)	O28 Gd1 O11 116.67(11)	O11 Gd2 O35 145.40(13)

O11 Gd2 O36 84.03(13)	O35 Gd2 O36 73.56(14)	O11 Gd2 O12 74.64(12)
O35 Gd2 O12 74.30(13)	O36 Gd2 O(12) 74.99(12)	O11 Gd2 O19 75.79(12)
O35 Gd2 O19 138.12(13)	O36 Gd2 O19 135.91(13)	O12 Gd2 O19 133.33(12)
O11 Gd2 O29 80.04(12)	O35 Gd2 O29 114.51(13)	O36 Gd2 O29 69.24(12)
O12 Gd2 O29 137.82(12)	O19 Gd2 O29 68.89(12)	O11 Gd2 O30 129.46(11)
O35 Gd2 O30 78.90(13)	O36 Gd2 O30 93.57(13)	O12 Gd2 O30 152.87(12)
O19 Gd2 O30 71.49(12)	O29 Gd2 O30 52.74(12)	O11 Gd2 O(1) 123.46(12)
O35 Gd2 O1 74.15(13)	O36 Gd2 O1 147.68(13)	O12 Gd2 O1 94.88(12)
O19 Gd 2O1 72.83(12)	O29 Gd2 O1 127.29(12)	O30 Gd2 O1 81.66(11)
O11 Gd2 O2 74.53(11)	O35 Gd2 O2 107.65(13)	O36 Gd2 O2 141.77(12)
O12 Gd2 O2 69.03(11)	O19 Gd2 O2 68.77(11)	O29 Gd2 O2 134.62(12)
O30 Gd2 O2 124.51(11)	O1 Gd2 O2 50.63(11)	O(2) Gd(1) O(38) 144.24(12)

1b

Gd(1)-O(20) 2.304(4)	Gd(1)-O(10) 2.333(4)	Gd(1)-O(16) 2.354(5)
Gd(1)-O(17) 2.374(3)	Gd(1)-O(1W) 2.406(6)	Gd(1)-O(1) 2.430(4)
Gd(1)-O(3W) 2.433(4)	Gd(1)-O(2W) 2.457(4)	

O(20)-Gd(1)-O(10)	82.09(14)	O(20)-Gd(1)-O(16)	142.56(18)
O(10)-Gd(1)-O(16)	118.75(19)	O(20)-Gd(1)-O(17)	98.55(13)
O(10)-Gd(1)-O(17)	145.52(15)	O(16)-Gd(1)-O(17)	81.23(19)
O(20)-Gd(1)-O(1W)	144.73(17)	O(10)-Gd(1)-O(1W)	79.07(19)
O(16)-Gd(1)-O(1W)	72.6(2)	O(17)-Gd(1)-O(1W)	81.32(19)
O(20)-Gd(1)-O(1)	71.86(13)	O(10)-Gd(1)-O(1)	138.72(14)
O(16)-Gd(1)-O(1)	72.69(18)	O(17)-Gd(1)-O(1)	71.54(14)

O(1W)-Gd(1)-O(1)	138.48(17)	O(20)-Gd(1)-O(3W)	80.66(13)
O(10)-Gd(1)-O(3W)	71.62(13)	O(16)-Gd(1)-O(3W)	77.86(18)
O(17)-Gd(1)-O(3W)	142.75(13)	O(1W)-Gd(1)-O(3W)	120.26(19)
O(1)-Gd(1)-O(3W)	72.95(13)	O(20)-Gd(1)-O(2W)	74.67(12)
O(10)-Gd(1)-O(2W)	72.71(13)	O(16)-Gd(1)-O(2W)	138.80(18)
O(17)-Gd(1)-O(2W)	74.26(12)	O(1W)-Gd(1)-O(2W)	71.38(18)
O(1)-Gd(1)-O(2W)	127.00(13)	O(3W)-Gd(1)-O(2W)	138.81(12)

1c

Gd(1)-O(1) 2.302(5)	Gd(1)-O(13) 2.357(5)	Gd(1)-O(2W) 2.370(6)
Gd(1)-O(2) 2.378(5)	Gd(1)-O(20) 2.394(7)	Gd(1)-O(12) 2.418(4)
Gd(1)-O(1W) 2.425(5)	Gd(1)-O(3W) 2.466(4)	

O(1)-Gd(1)-O(13)	81.57(19)	O(1)-Gd(1)-O(2W)	146.6(2)
O(13)-Gd(1)-O(2W)	72.3(3)	O(1)-Gd(1)-O(2)	100.44(17)
O(13)-Gd(1)-O(2)	146.00(18)	O(2W)-Gd(1)-O(2)	90.5(3)
O(1)-Gd(1)-O(20)	142.0(2)	O(13)-Gd(1)-O(20)	121.2(2)
O(2W)-Gd(1)-O(20)	71.1(3)	O(2)-Gd(1)-O(20)	77.6(2)
O(1)-Gd(1)-O(12)	72.01(17)	O(13)-Gd(1)-O(12)	138.2(2)
O(2W)-Gd(1)-O(12)	141.2(3)	O(2)-Gd(1)-O(12)	72.16(18)
O(20)-Gd(1)-O(12)	71.3(2)	O(1)-Gd(1)-O(1W)	83.1(2)
O(13)-Gd(1)-O(1W)	71.28(17)	O(2W)-Gd(1)-O(1W)	106.9(3)
O(2)-Gd(1)-O(1W)	142.69(17)	O(20)-Gd(1)-O(1W)	77.5(2)
O(12)-Gd(1)-O(1W)	73.83(18)	O(1)-Gd(1)-O(3W)	75.49(15)
O(13)-Gd(1)-O(3W)	72.41(16)	O(2W)-Gd(1)-O(3W)	77.0(2)

O(2)-Gd(1)-O(3W)	75.29(17)	O(20)-Gd(1)-O(3W)	137.5(2)
O(12)-Gd(1)-O(3W)	128.05(15)	O(1W)-Gd(1)-O(3W)	139.97(17)

Table S2. Crystal and Structure Refinement Data for 1, 1a, 1b and 1c.

Compound	**1**	**1a**
empirical formula	$C_{66}H_{68}Gd_2N_{20}O_{47}$	$C_{73}H_{73}ClGd_2N_{20}O_{45}$
formula wt	2207.90	2300.46
Temperature	100K	100K
Radiation	MoK_α	MoK_α
Wavelength	0.71073	0.71073
crystal system	Monoclinic	Monoclinic
space group	*P*21/n	*P*21/n
a, Å	13.103(4)	13.137(5)
b, Å	30.424(6)	30.227(5)
c, Å	23.434(5)	23.326(5)
α (°)	90.000	90.000
β (°)	101.392(5)	102.075(5)
γ (°)	90.000	90.000
U, Å^3	9158(4)	9058(4)
Z	4	4
ρ_{calc}, g/cm^3	1.601	1.687
μ, mm^{-1}	1.543	1.591
F(000)	4432	4624
refl.collected	46632	61950
R_{int}	0.0583	0.0426
independent refl.	16077	16840
Refinement method	Full-matrix least-squares on F^2	Full-matrix least-squares on F^2
GOF	1.056	1.042
final *R* indices [I>2σ (*I*)]	R1 = 0.0502 wR2 = 0.1256	R1 = 0.0445 wR2 = 0.1051
R indices (all data)	R1 = 0.0659 wR2 = 0.1386	R1 = 0.0599 wR2 = 0.1137

Compound	**1b**	**1c**
empirical formula	$C_{34}H_{37}FGdN_8O_{27}$	$C_{38}H_{42}GdN_9O_{26}$
formula wt	1165.94	1198.03
Temperature	100K	100K
Radiation	MoK_α	MoK_α
Wavelength	0.71073	0.71073
crystal system	Monoclinic	Monoclinic
space group	*C*2/c	*C*2/c
a, Å	25.179(5)	25.466(5)
b, Å	14.747(5)	14.961(5)
c, Å	26.053(5)	26.140(5)
α (°)	90.000	90.000
β (°)	94.964	94.842(5)
γ (°)	90.000	90.000
U, Å^3	9638(4)	9924(4)
Z	8	8
ρ_{calc}, g/cm^3	1.590	1.593
μ, mm^{-1}	1.477	1.433
F(000)	4592	4776
refl.collected	33262	25478
R_{int}	0.0412	0.0930
independent refl.	8924	8722
Refinement method	Full-matrix least-squares on F^2	Full-matrix least-squares on F^2
GOF	1.035	1.026
final *R* indices [I>2σ (*I*)]	R1 = 0.0626 wR2 = 0.1607	R1 = 0.0831 wR2 = 0.2172
R indices (all data)	R1 = 0.0930 wR2 = 0.1834	R1 = 0.1222 wR2 = 0.2520

Table S3. Selected non-covalent interactions of **1.**

Interaction	H···A (Å)	D–H···A (deg.)
C57-H57A···O29	3.0375(49)	142.948(56)
C66-H66C···O34	3.6462(56)	135.397(44)
C58-H58···N17	3.3977(71)	161.675(46)
C66-H66A···O27	2.8224(42)	153.601(42)
C10-H10···O44	3.599(39)	142.575(39)
C59-H59B···N20	3.582	142.801

Table S4. Selected non-covalent interactions in **1a.**

Interaction	H···A (Å)	D–H···A (deg.)
C52-H52A···O43	3.182(11)	120.383(42)
C68-H68···N20	3.4389(71)	151.143(65)
C67-H67···O3	2.9042(46)	119.69(72)
C70-H70···O31	3.3139(61)	148.151(59)
C71-H71···O32	2.6176(77)	131.926(64)
C67-H67···O8	3.1512(53)	161.429(71)
C64-H64A···O27	2.9298(52)	160.469(72)
C65-H65A···O27	2.7382(59)	170.362(61)

Table S5. Selected non-covalent interactions in **1b**

Interaction	H···A (Å)	D–H···A (deg.)
C25-H25···O2	2.5569(39)	135.669(88)
C26-H26···O6	2.3903(88)	126.314(14)
C29-H29···O3	2.7458(43)	130.109(49)
C29-H29···N1	2.8801(49)	129.243(50)
C22-H22B···F	2.4483(4)	149.693(72)

Table S6. Selected non-covalent interactions in **1c.**

Interaction	H···A (Å)	D–H···A (deg.)
C24-H24···O11	2.5702(52)	148.149(670)
C25-H25···O12	3.0200(47)	143.953(93)
C27-H27A···O3W	2.896(47)	152.743(97)
C27-H27A···O2W	3.0346(81)	127.027(168)
C32-H32···O9	2.5631(54)	119.559(118)
C28-H28···O10	2.5956(52)	151.585(118)

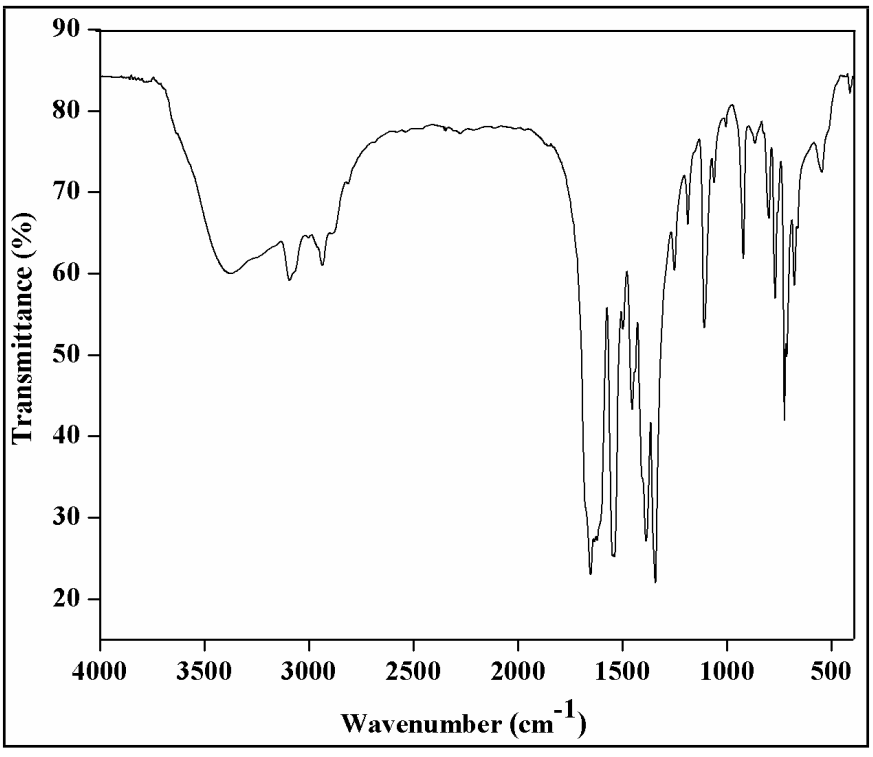

Fig. S1. FT-IR spectrum of **1**.

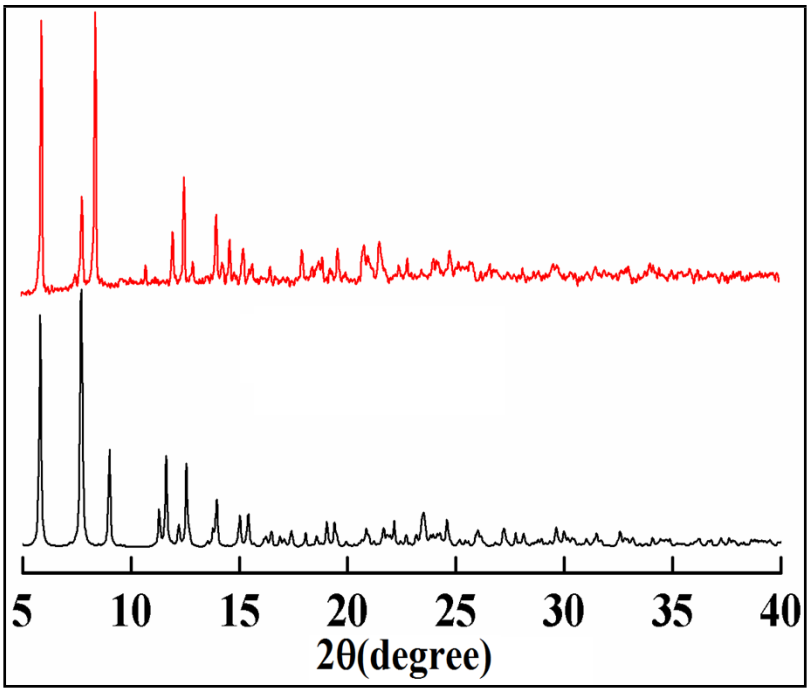

Fig. S2. PXRD patterns of **1**. Bottom: simulated, top: as-synthesized.

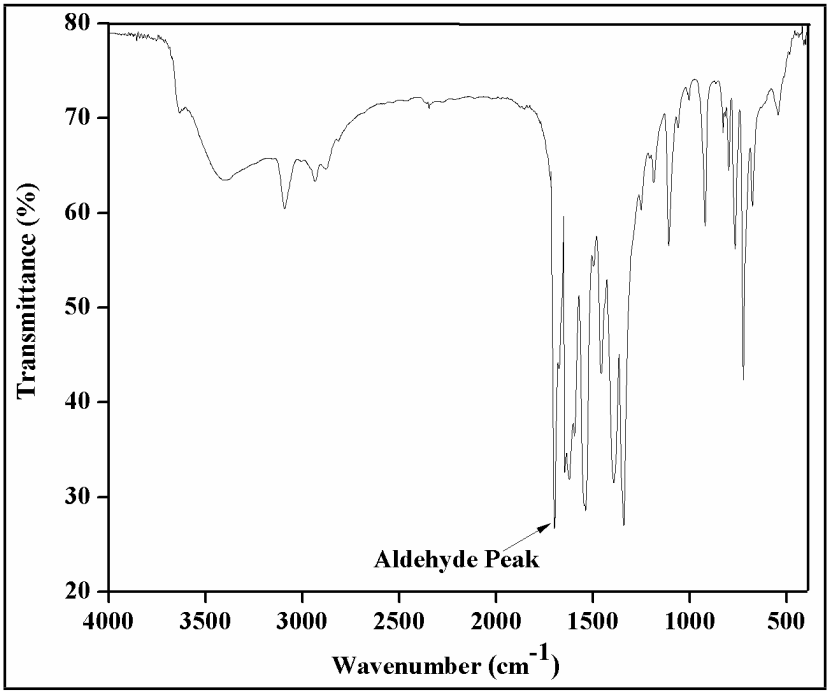

Fig. S3. FT-IR spectrum of **1a**

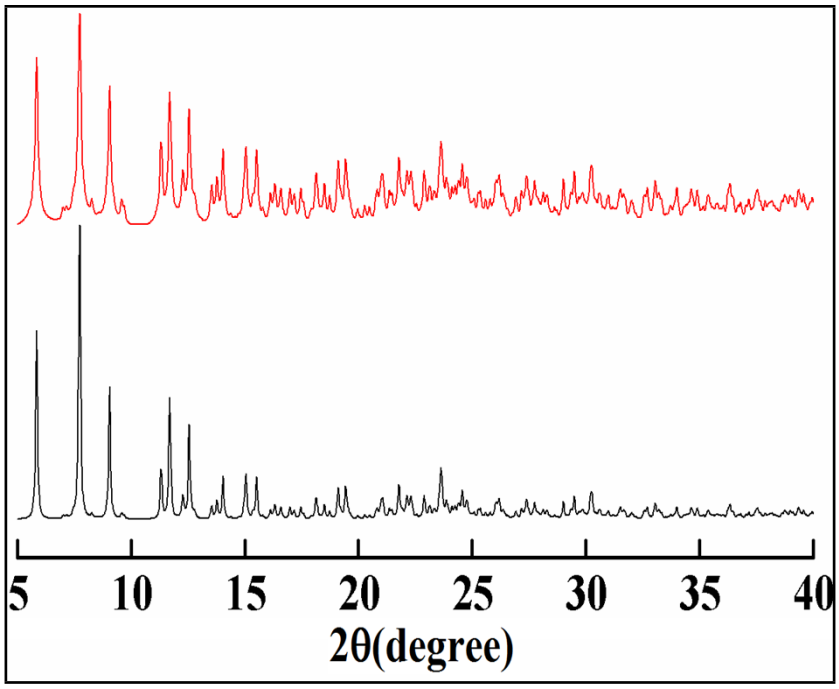

Fig. S4. PXRD patterns of **1a**. Bottom: simulated, top: as-synthesized.

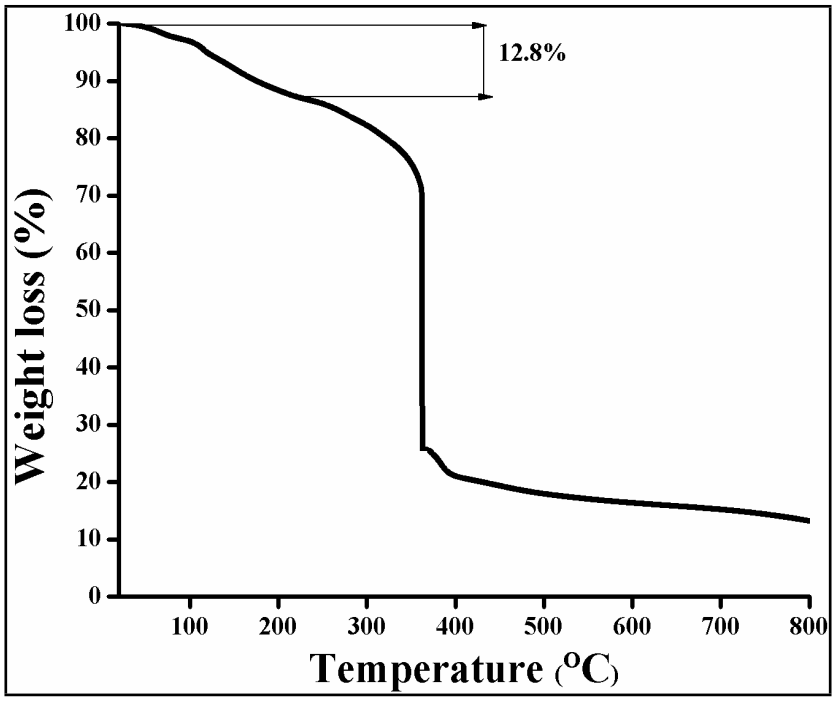

Fig. S5. Thermogravimetric curve of **1a**.

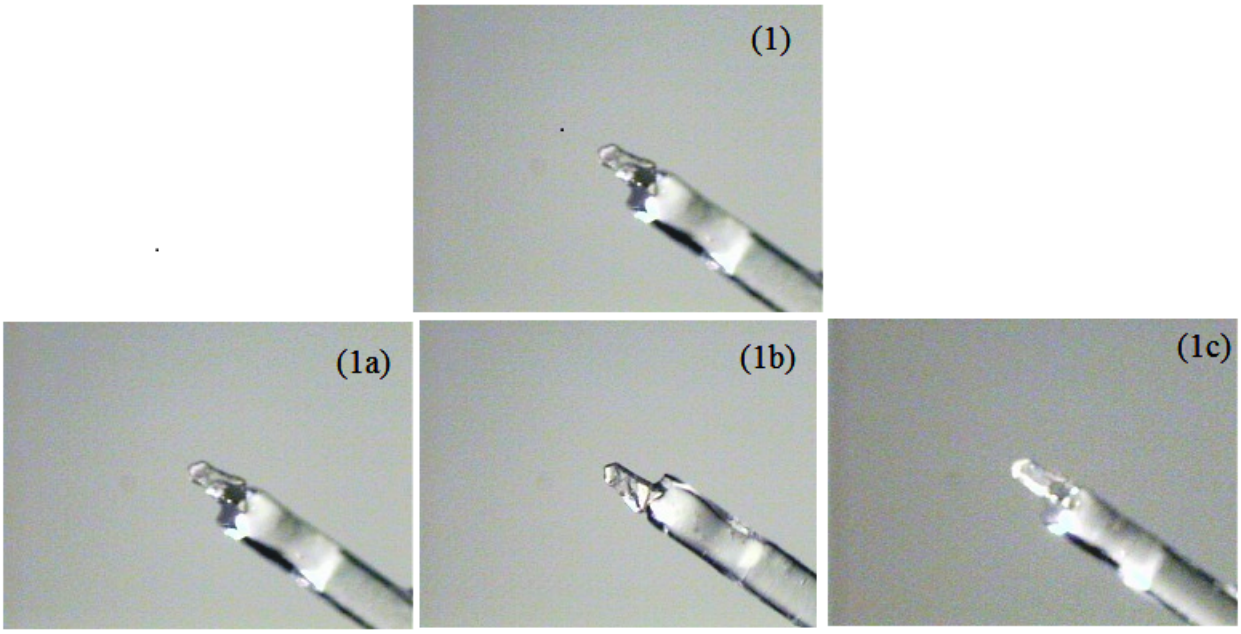

Fig. S6. Photographs of single crystals of **1**, **1a**, **1b** and **1c**.

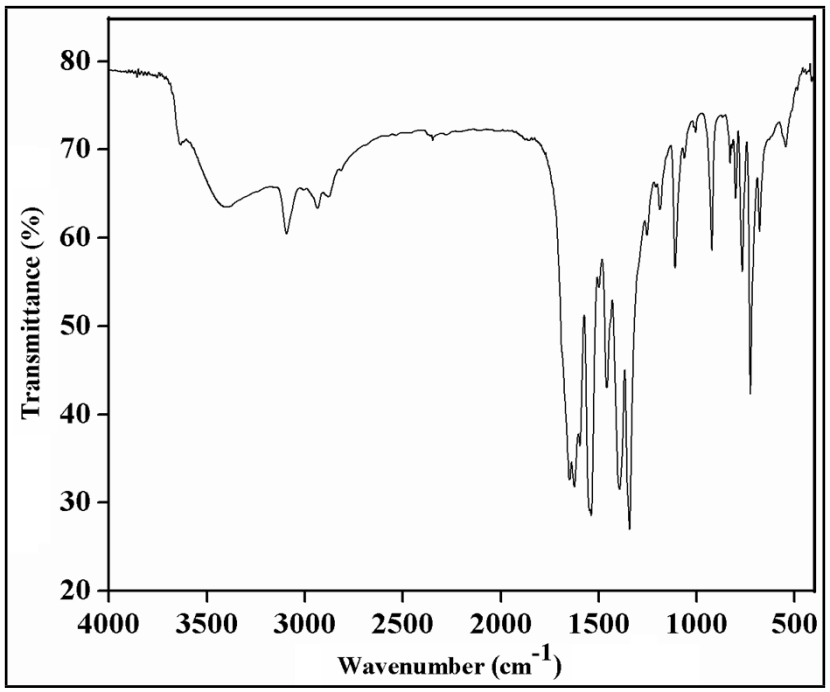

Fig. S7. FT-IR spectrum of regenerated **1**, obtained from **1a**.

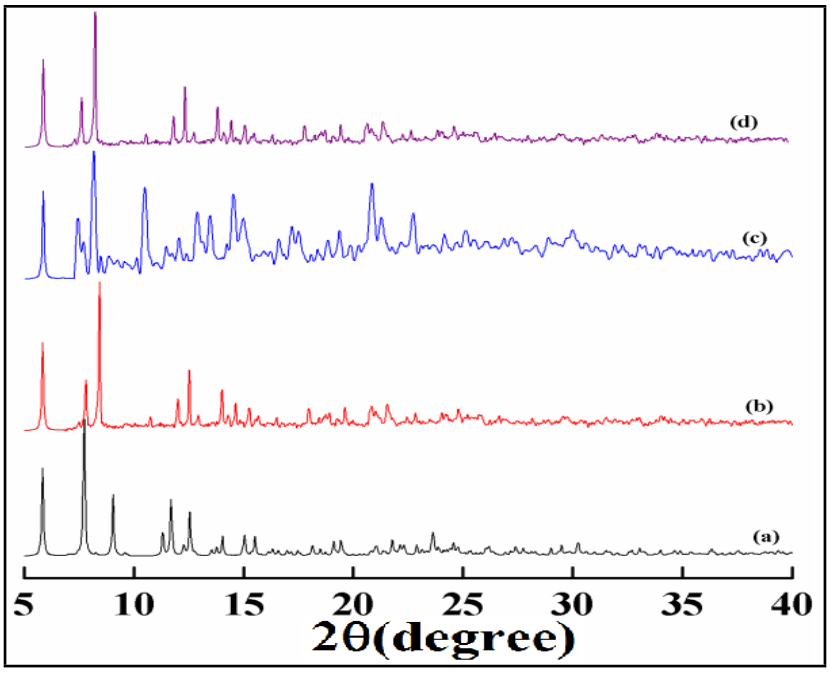

Fig. S8. PXRD patterns of (a) simulated of **1**, (b) regenerated of **1** from **1a**, (c) regenerated of **1** from **1b** and (d) regenerated of **1** from **1c**.

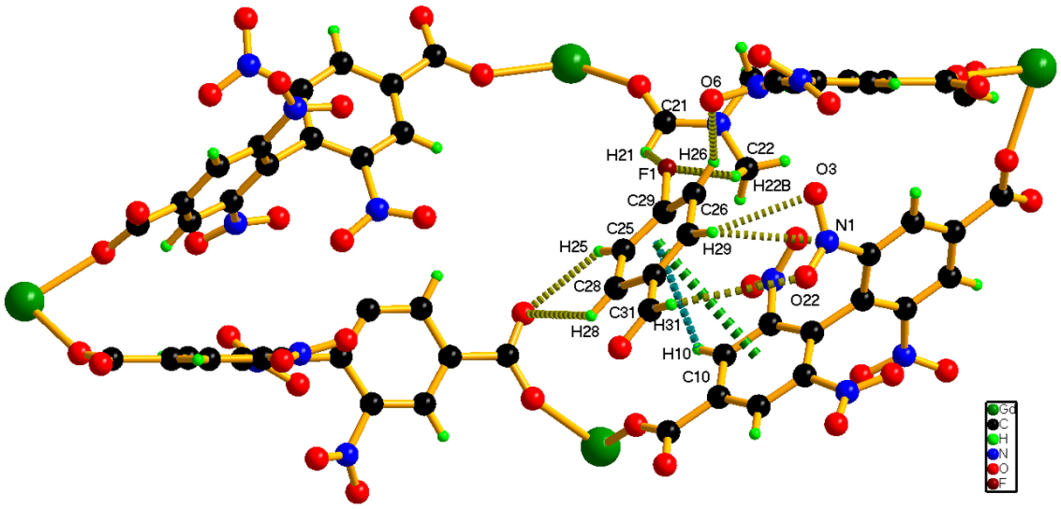

Fig. S9. View of the H-bonding interactions between guest 4-fluorobenzaldehyde molecule and the host framework inside pore A of **1b**.

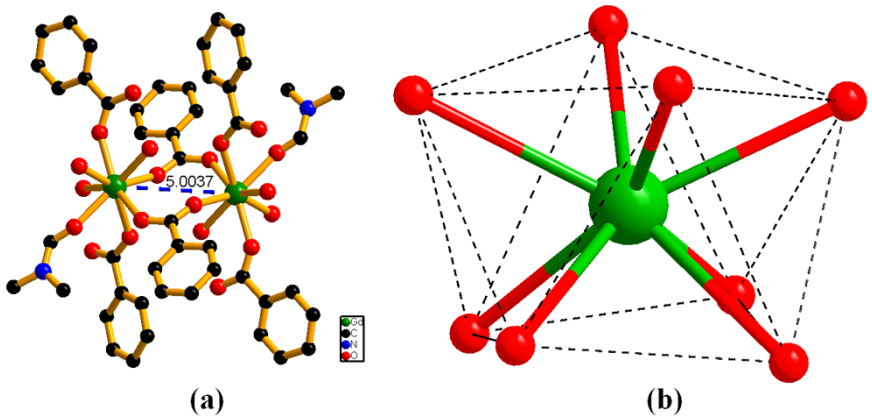

Fig. S10. Perspective views of (a) coordination environment around the Gd_2 dimer in compound **1c**, and (b) geometry around metal center (hydrogen atoms are omitted for clarity).

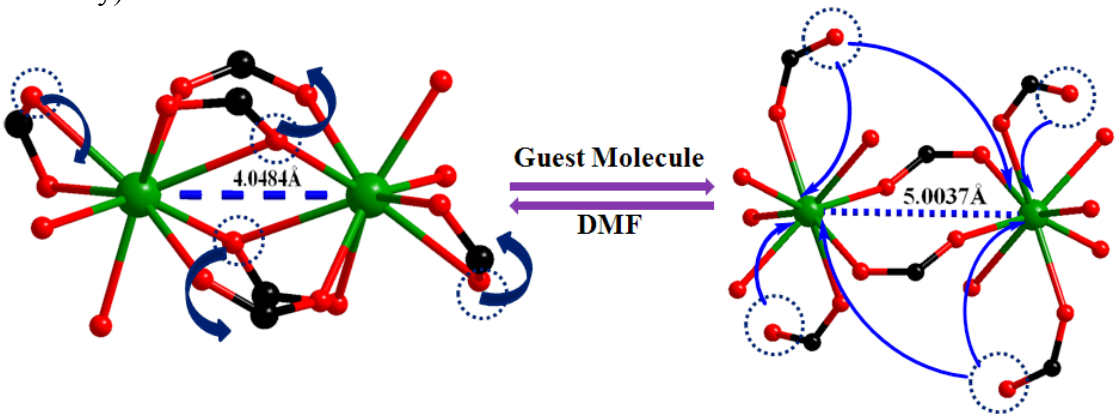

Fig. 11. Schematic representation of the bonding rearrangement, including carboxylate shift processes, that occur during the reversible SC-SC transformation between **1** and **1c**.

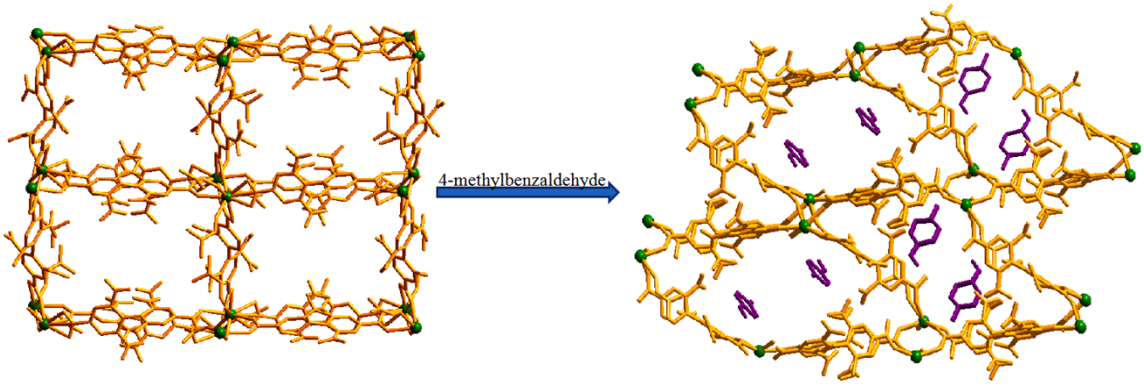

Fig. 12. Schematic view of the single-crystal to single-crystal guest-exchange process, followed by extensive channel rearrangement, in **1c**.

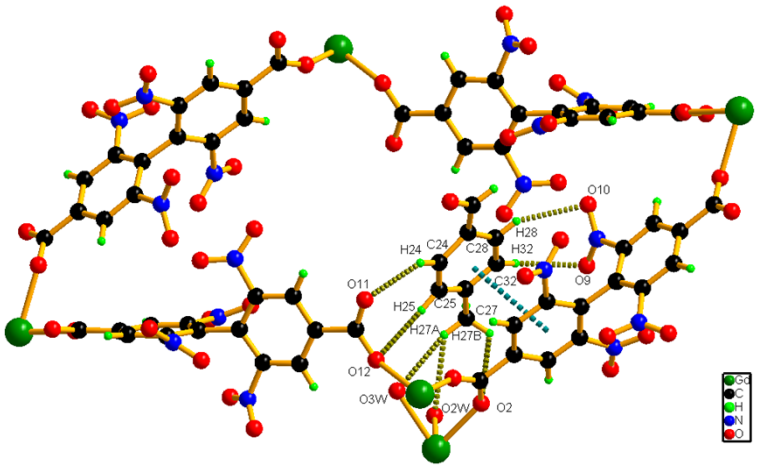

Fig. S13. View of the H-bonding interactions of guest 4-methylbenzaldehyde molecule with the host framework inside the pore A of **1c**.

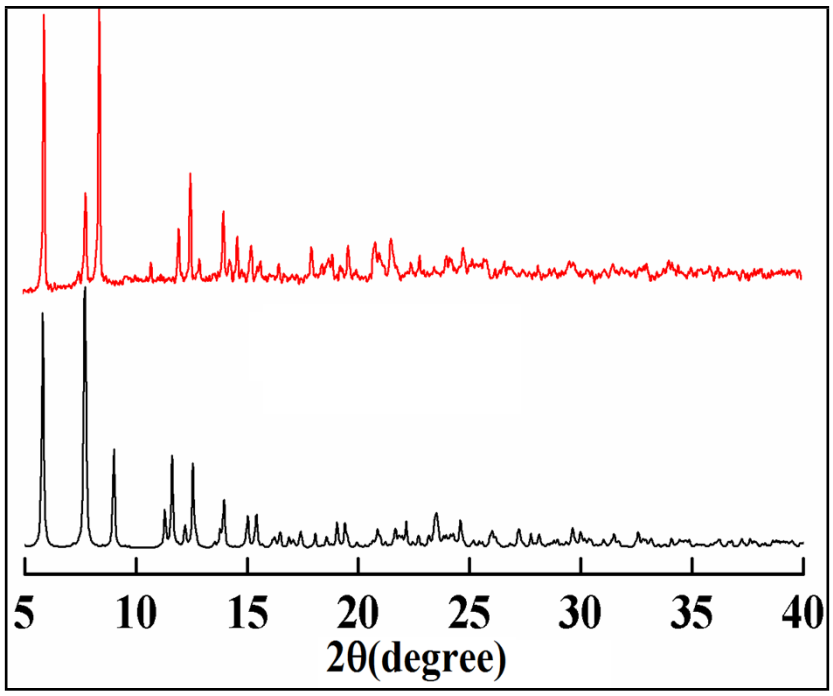

Fig. S14. PXRD patterns of **1b**, bottom: simulated, top: as-synthesized.

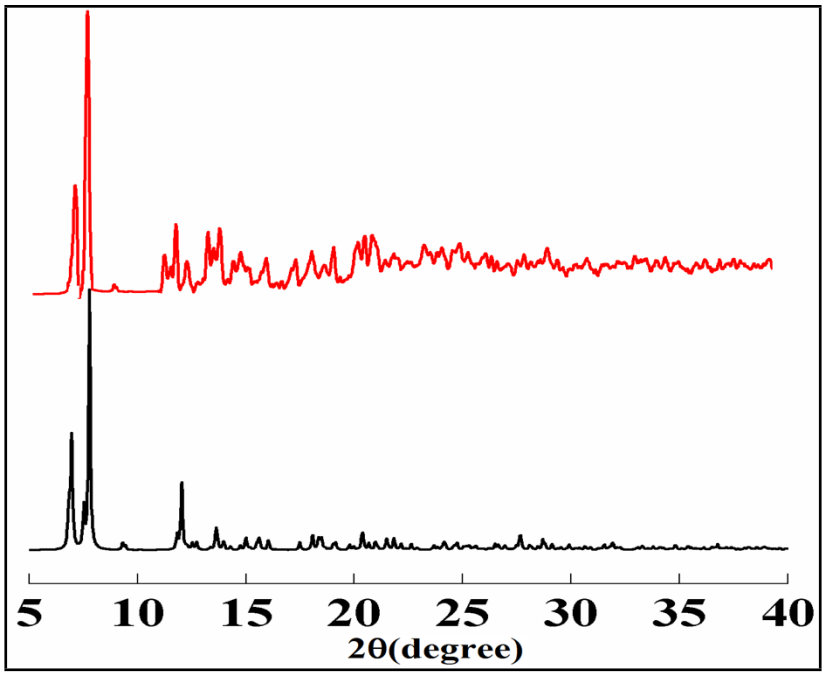

Fig. S15. PXRD patterns of **1c**, bottom: simulated, top: as-synthesized.

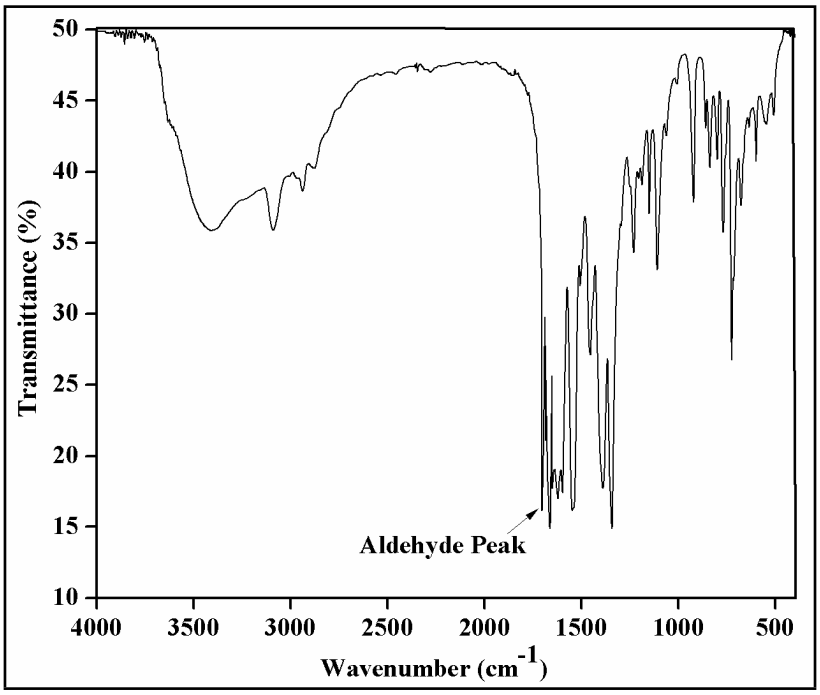

Fig. S16. FT IR spectrum of **1b**.

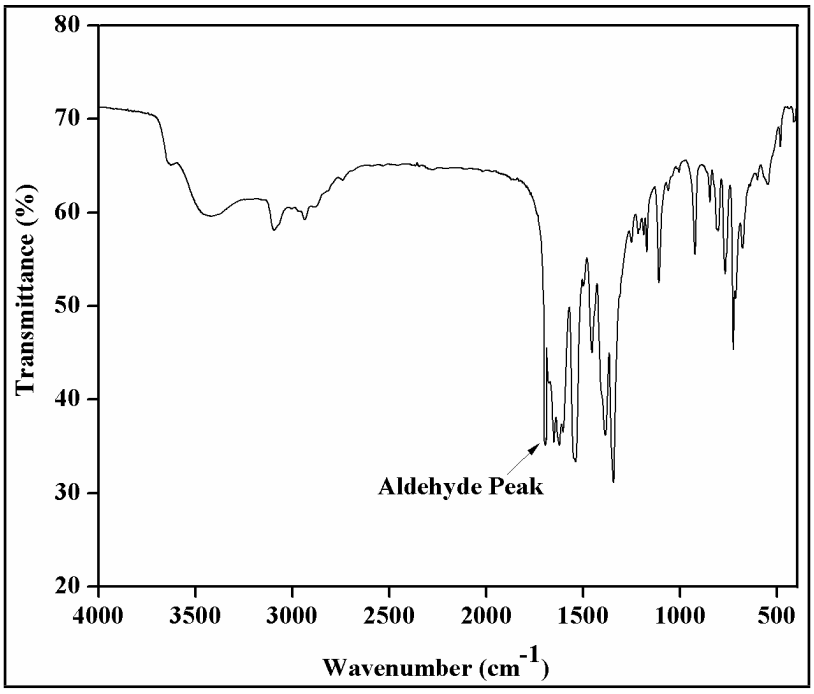

Fig. S17. FT IR spectrum of **1c**.

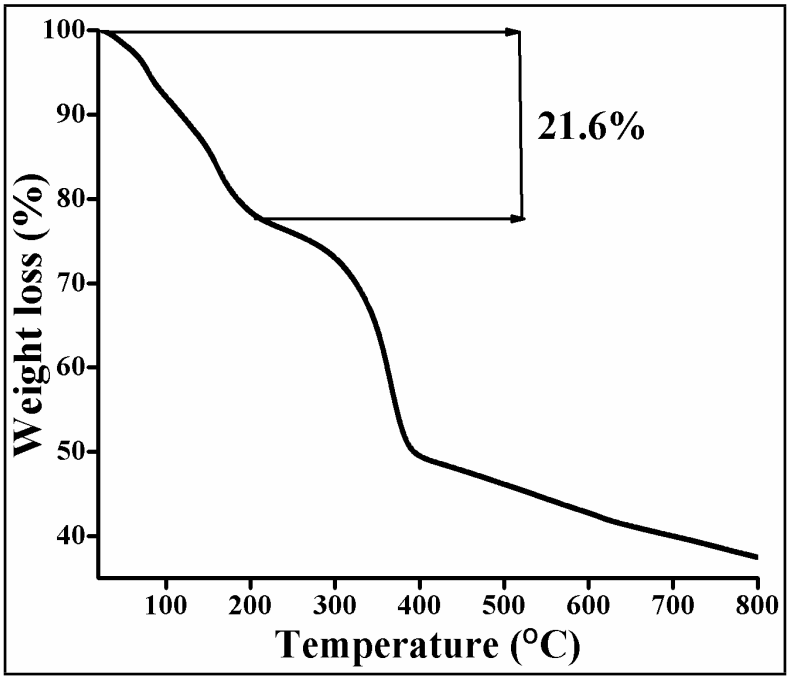

Fig. S18. Thermogravimetric analysis of **1b**.

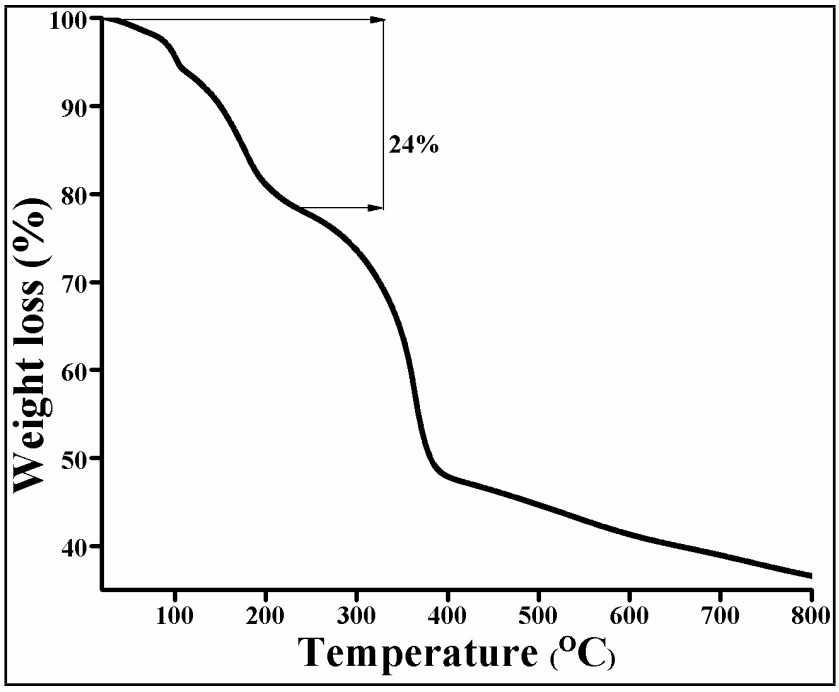

Fig. S19. Thermogravimetric analysis of **1c**.

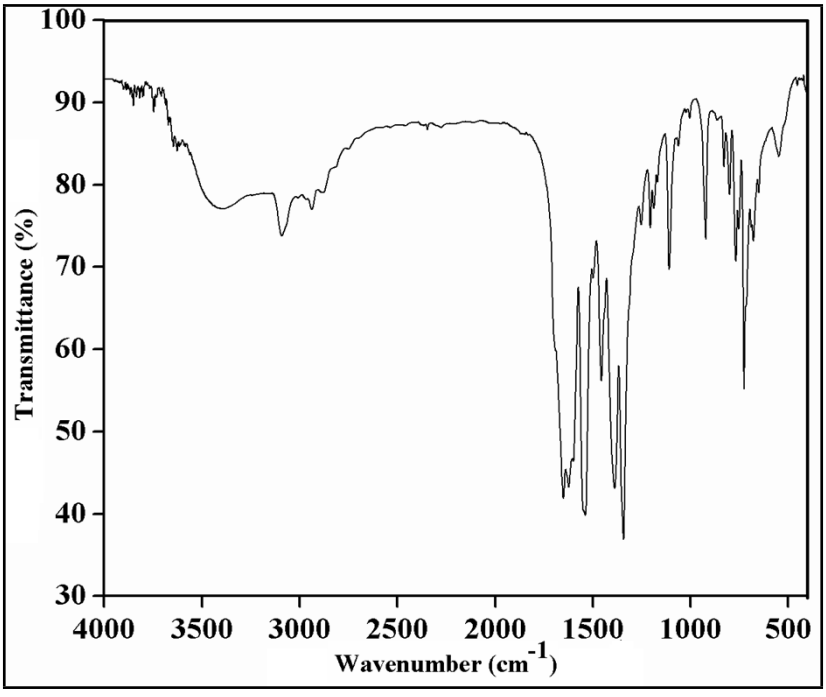

Fig. S20. FT IR spectrum of regenerated, **1** from **1b**.

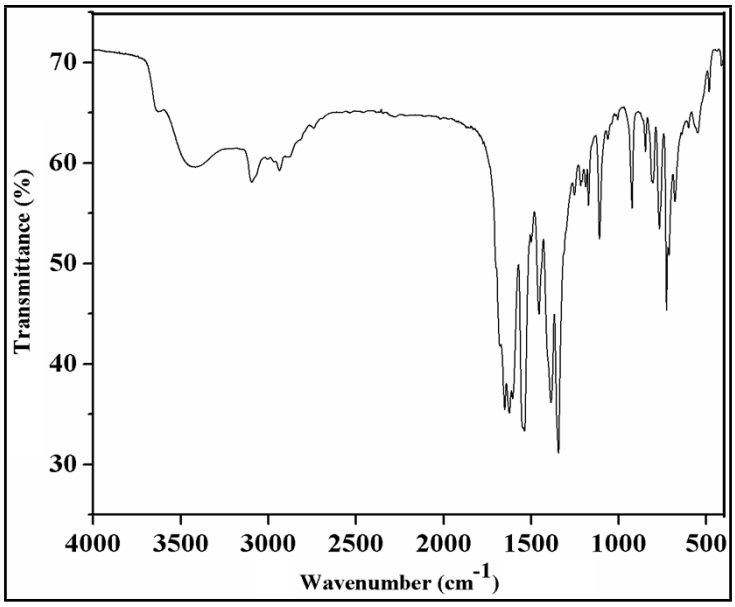

Fig. S21. FT IR spectrum of regenerated, **1** from **1c**.

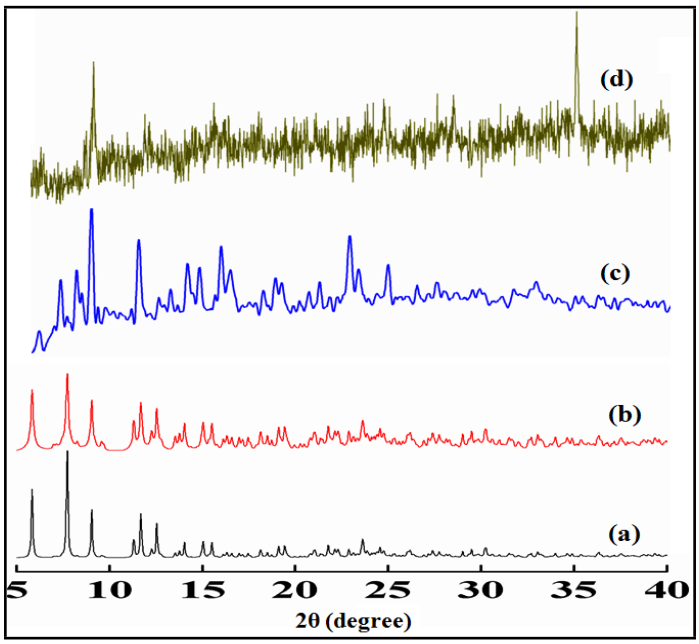

Fig. S22. PXRD patterns of guest 4-chlorobenzaldedhyde (4-ClPhCHO) loading cycles for **1a**: (a) simulated, (b) after cycle 1, (c) after cycle 2, (d) after cycle 3. PXRD pattern of (d) indicates complete collapse of the framework.

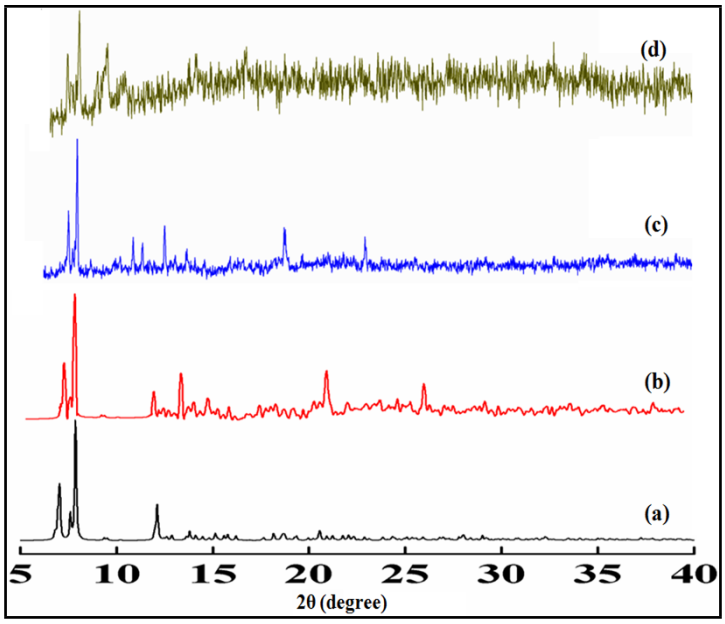

Fig. S23. PXRD patterns of guest 4-fluorobenzaldehyde (4-FPhCHO) loading cycles for **1b**: (a) simulated, (b) after cycle 1, (c) after cycle 2, (d) after cycle 3. PXRD pattern of (d) indicates complete collapse of the framework.

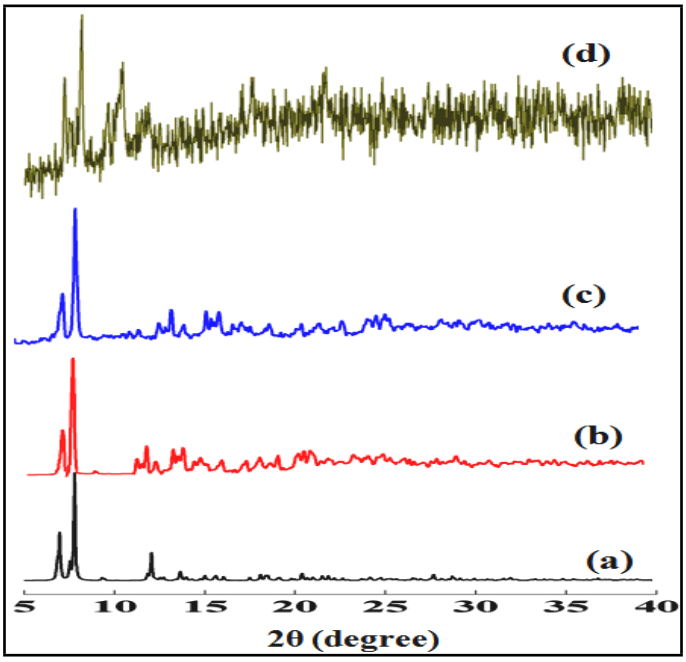

Fig. S24. PXRD patterns of guest 4-methylbenzaldehyde (4-MePhCHO) loading cycles for **1c**: (a) simulated, (b) after cycle 1, (c) after cycle 2, (d) after cycle 3. PXRD pattern of (d) indicates complete collapse of the framework.